Advances in Military Technology
Vol. 19, No. 1, 2024, pp. 71-90
ISSN 1802-2308, eISSN 2533-4123
DOI 10.3849/aimt.01870

Comparison of Penetration Capability of Several Contemporary 5.56 × 45 mm Projectiles into Hard Targets

A. Catovic*

Mechanical Engineering Faculty, University of Sarajevo, Bosnia and Herzegovina

The manuscript was received on 28 November 2023 and was accepted after revision for publication as technical information on 26 March 2024.

Abstract:

The analysis was performed on six commonly used 5.56 × 45 mm projectile types (M193, M855, M855A1, L31A1, M995, and AP45). The projectile's impact velocity (chosen as 900 m/s) was the same in the examination process. This made it possible to assess how the projectile's design has affected its performance against a hard steel target. These evaluations included numerical simulations (Ansys Autodyn) of projectile impacts. Using the available experimental data, the materials in the computational model were first validated. A short description and CAD model of projectiles is also given. Relevant conclusions were reported.

Keywords:

small-caliber ammunition, 5.56 × 45 mm, penetration, terminal ballistics, simulation

1 Introduction

Worldwide, small-caliber projectiles are frequently employed in both military and non-military contexts. The 5.56 × 45 mm NATO is a family of intermediate cartridges with a bottleneck and rimless design, created in Belgium by FN Herstal in the late 1970s. In 1980, it was standardized under STANAG 4172 as the second standard service rifle cartridge for both NATO and non-NATO forces. The 5.56 × 45 mm NATO cartridge family was developed from the 223 Remington cartridge, which Remington Arms produced in the early 1960s. Although they are not identical, they are similar in some parameters. The creation of a new lightweight combat rifle would be inextricably related to the development of the cartridge that would later become the .223 Remington, from which 5.56 mm NATO would finally be designed. The study is divided into

* *Corresponding author: University of Sarajevo, Mechanical Engineering Faculty, Defense Technology Department, Vilsonovo setaliste 9, BA 71000 Sarajevo, Bosnia and Herzegovina. Phone: 00387 61 70 92 52, E-mail: catovic@mef.unsa.ba. ORCID 0000-0002-3599-4143.*

a couple of sections: a review of the literature, a description of the projectiles that were employed, a validation of the numerical model, and a section on numerical simulation with analysis and conclusions.

2 Review of Research

Studies on the penetrating capability of small-caliber ammunition are numerous. Leeder [1] investigated projectiles with standard dimensions and sintered tungsten carbide cores, both in .30 and .50 calibers. They were tested in normal and oblique impact firings against uniform, face-hardened armor plates. When compared to standard AP projectiles, the carbide projectiles showed a significantly higher penetration ability at normal impact for a given energy. However, at obliquities, the carbide projectiles' penetration ability declined more quickly than the AP projectiles' at normal impact. The sharp transition in the obliquity behavior of the carbide projectiles against both plates is associated with the relative weaknesses of these hard-sintered materials to transverse impact, all cores tending to shatter or pulverize although still retaining sufficient toughness to surpass the standard AP projectiles cores at angles up to 30° against face-hardened plate. Hazell et al [2] simulated projectile 5.56 × 45 mm SS109 using Autodyn, to provide insight into the penetration mechanics regarding the higher residual velocity of this projectile when striking an inclined target plate compared to normal impact, with effective path lengths being the same. A 7.62 mm APM2 projectile fired in the 775-950 m/s velocity range was used to estimate the ballistic performance of metallic plates that were monolithic, double- or triple-layered, and composed of steel, aluminum, or a combination of these materials by Flores-Johnson et al. [3]. The explicit FEM code LS-DYNA was utilized.

Kılıç [4] estimated the ballistic limit for a 7.62 mm 54R B32 API hardened steel core projectile against armor steel (500 HB). The 3D Lagrange and smoothed particle hydrodynamics numerical simulations were performed. Kılıç et al. [5] used a hybrid approach to estimate the ballistic limit thickness for armor steels by combining FEM simulation with artificial neural network analysis.

Penetration depth tests and numerical simulations of the 5.56 × 45 mm SS109 projectile impact into passive, layered armor, positioned on the armor backing material, were carried out by Wiśniewski [6]. As a result, the best armor for deterring the SS109 projectile was presented. Hazell [7] used Autodyn to simulate penetration of projectile 5.56 mm L2A2 into AISI 1040 steel plate, termically treated to different values of hardness.

The study conducted by Janiszewski et al. [8] examined the effects of 7.62 mm AP projectiles on high-strength steel plates (30PM steel). The collected experimental data can be valuable as a reference for assessing various models and numerical approaches accessible in hydrocodes that are sold commercially. Coghe et al [9] investigated the bodywork effect - a phenomenon in which the addition of extra armor does not lead to a higher level of protection. They conducted dynamic characterization of the armor material and also performed numerical simulations, as well as an analytical residual velocity approach (Recht - Ipson model).

An interesting overview of the materials (used in Russia and Western countries) utilized for projectile cores and penetrators was provided by Kolmakov et al. [10]. They recommended using high-carbon low-alloy steels with a hardness of around 70 HRC and a natural composite structure for high-penetration, mass-produced components. When it comes to materials for the cores of special-purpose armor-piercing

projectiles, high-speed steels with a high bending strength that are sparingly alloyed are the ideal substitutes for tungsten alloys. Chromium-tungsten WD 74100 steel with a hardness of 65 HRC was earlier used to make the cores of US AP projectiles for the 12.7 × 99 mm NATO AP M2 and M8 cartridges. Eventually, less rare manganese-molybdenum FXS318 alloy steel was used to make the cores of AP M2 projectiles. Its hardness ranged from 61 to 64 HRC after quenching. 7.62 mm AP M2 and 12.7 mm AP M2 projectiles' AP cores were likewise made of high-hardness steel and martensitic alloy steel with a hardness of 570-640 HB (≈57-59 HRC). The projectile cores for cartridges made of 7.62 × 51 mm by Hirtenberger Patronenfabrik, 7.62 × 51 mm AP by Fabrique Nationale, and 7.62 × 63 mm (.30-06 M2 AP) by US Government Arsenal are constructed of alloy steel, which is composed similarly to high-speed steel. The alloy steel has a hardness of 750-785 HV (62-63 HRC). The 4340 alloy steel projectile, which has an ultimate tensile strength of 745 MPA and a hardness of 17 HRC, is also used in 7.62 × 51 mm NATO ammunition. Large-caliber AP projectiles for 12.7 × 99 mm NATO cartridges and similar projectiles contain AP cores produced of quenched tool low-alloy high-carbon 100Cr6 steel, which has an ultimate tensile strength of 1 100-1 300 MPa and a hardness of 60-64 HRC. This steel is comparable to both Russian ShKh15 and US 52100 steel. It is stated that for blunt AP cores, 100MnCrW4 alloy tool steel with a hardness of 53 HRC is used. The low-carbon, quenched 1007 steel is used to make the cores of the 7.62 × 63 mm Mauser AP projectiles. For the standard 7.62 × 51 mm rifle-machine gun cartridge, NATO uses a relatively short cylindrical core and a conical head made of a WC-Co alloy with a hardness of 1 450 HV (≈74 HRC) to make the Bofors FFV (Sweden) and M993 (United States) projectiles. A WC-based hard alloy AP projectile with a 5.6 mm diameter core is also utilized for the same standard NATO cartridge [10].

The impact deformation and fracture behavior of AP projectiles made with three different tool steel cores were examined by Di Benedetto et al [11]. They concluded that the ballistic efficacy of projectiles against armor made of hardened steel is directly linked to the hardness of their cores. According to research by Anderson et al. [12], the ballistic effectiveness of five distinct but unspecified types of hard steel projectiles increased with their hardness in the 200-750 HV range at impact velocities between 1 250 and 1 350 m/s. Tria [13] presented a new method to experimentally verify constitutive models and numerical models used in small arms ammunition terminal ballistics. In a study conducted by Rosenberg [14], the ballistic limit velocities of 7.62 mm AP M2 projectiles for different aluminum alloys were compared with experimental results and predictions from a previous numerical model. They included an empirical correction factor to take into consideration the impact of the projectiles' strong steel cores surrounded by a brass jacket.

Using computational analysis and forward/reverse ballistic techniques, Hazell et al. [15] examined the impact of the gilding jacket on the penetration of ceramic-faced objects by a 7.62 × 51 mm FFV AP projectile. Børvik et al. [16] investigated the perforation resistance of five different high-strength steels (Weldox 500E, Weldox 700E, Hardox 400, Domex Protect 500, and Armox 560T). Dey et al. [17] have examined the ballistic perforation resistance of monolithic and double-layered Weldox 700E steel plates struck by blunt and ogival projectiles based on numerous full-scale impact tests and corresponding numerical simulations using the explicit solver in LS-DYNA. Mohotti [18] analyzed the penetration of 5.56 × 45 mm projectile through aluminum-polyurea composite layered plate systems (different thicknesses) using an analytical

model and validated results with experiments and numerical simulations (LS Dyna). They concluded that polyurea reduces the residual velocity of projectiles.

The 7.62 × 54R projectile, hitting plates made of steel (HARDOX 450), aluminum alloy 7039, and titanium alloy Ti-6Al-4V was simulated in 2D and 3D numerically by Hub [19]. Soydan et al [20] conducted experimental testing and numerical simulation of ballistic impact of 9 mm FMJ projectile into laminated armor consisting of three layers of different materials: fiber-cement, Kevlar fabric, and steel. Siriphala [21] investigated (using Eulerian approach) Armox 600T target plate penetration when impacted by projectile of the 5.56 × 45 mm M193 cartridge. A numerical examination of the influence of fracture criteria on the perforation of high-strength 30PM steel plates subjected to an AP projectile 7.62 × 51 mm was given by Tria [22]. Horsfall et al [23] fired four types of light-armor piercing projectiles (three types of 7.62 × 51 mm AP and the 30-06 AP M2 (7.62 × 63 mm) projectile) into mild steel, high-hardness steel and ceramic-faced composite armor targets. The ballistic limit velocity and the ballistic limit energy were assessed.

Kneubuehl [24] describes different effectiveness criteria for small-caliber projectiles when penetrating soft targets (i.e. traditional criteria based on projectile momentum, on projectile energy, and statistics-based criteria). He also describes projectiles with good penetration properties (high sectional density – heavy projectiles with small cross-sectional area) and projectiles designed for maximum effectiveness against soft targets (small sectional density – lower mass projectiles or projectiles which increase their surface such as deforming and fragmenting projectiles). Hub et al [25] performed an analysis of the terminal-ballistic behavior of a pistol projectile penetrating a block of substitute biological material. The penetration and perforation of Weldox 460 E steel plates with varying thicknesses, impacted by a blunt projectile at different impact velocities, were investigated experimentally, analytically, and numerically by Børvik et al. [26].

Yin et al [27] reported that the 88WC-12Co cores have a certain self-sharpening capability during the armor piercing process. Through testing, they looked at the armor piercing efficiency of 93W-4Ni-3Fe and 88WC-12Co cores with the same impact velocity and core size. Edwards [28] compared penetration capabilities (against tool steel targets of different hardness and heat treatment) of two 7.62 mm projectiles, one with blunted steel core (fine-grained ferrite-pearlite steel inside low carbon steel jacket) inside the gilding metal jacket and the other with tungsten carbide core (composition (weight percent): C 5.2, W 82.6, Co 10.5, Fe 0.41 of hardness 1200 HV) in the gilding metal jacket. In all cases there was an increase in ballistic limit velocity as the target hardness increased. The greater effect of plate hardness was noted for the softer penetrator (steel core projectile) due to the greater amount of deformation of these projectiles, reducing the kinetic energy density and the overall effectiveness.

Erzar [29] performed characterization of tungsten carbide (WC-Co, with 12 wt% Co) behavior at very high strain rates. This material is used in several small caliber armor piercing ammunitions. Mubashar et al [30] investigated (tests and simulations) performance of a perforated armor plate against a 12.7 mm AP-T projectile.

Morka [31] investigated a novel idea for ceramic backing in multilayer ballistic panels using AP 7.62 × 51 mm projectile type with a tungsten carbide core. The panel construction was composed of Al_2O_3 ceramic tile supported by a steel or aluminum alloy plate. Johnson [32] reports on tests of four types of tungsten carbide materials (WC cermets), with cobalt percentage from 3-15 %. Mechanical parameters of materi-

als are compared, with very high values of compressive strength and modulus of elasticity noticed.

The normal and oblique impact of 7.62 × 63 mm NATO balls and 7.62 × 63 mm AP M2 projectiles on 20 mm thick AA6082-T4 aluminum plates were studied (both mathematically and experimentally) by Børvik et al. [33]. The critical oblique angle at which the penetration process changes from perforation to embedment or ricochet was determined to be less than 60° for both projectile types. For the AP M2 projectiles, there was good agreement between the simulation and experimental results; however, for the soft core Ball projectiles, it was more challenging to produce consistent simulation results. Kılıç et al. [34] investigated the essential factors that stop the 7.62 × 54 mm armor-piercing projectile from penetrating the high hardness perforated plates through experiments and simulations. Projectiles can be defeated by three mechanisms: unequal pressures that cause the projectile to veer off course, projectile core fracture, and erosion of the projectile core nose.

3 Description of 5.56 × 45 mm Projectiles Used in the Research

The 5.56 × 45 mm NATO small caliber projectiles in various designs are the focus of this study. Due to the availability of material models experimental data [35], a projectile for 9 × 19 mm, Ball cartridge will also be used in the research during the projectile components material validation process. First of all, the projectiles will be described in this section. Three-dimensional model cross-sections of various 5.56 × 45 mm projectiles used in the study are displayed in Fig. 1. All 2D/3D models were created with the best data that was publicly available.

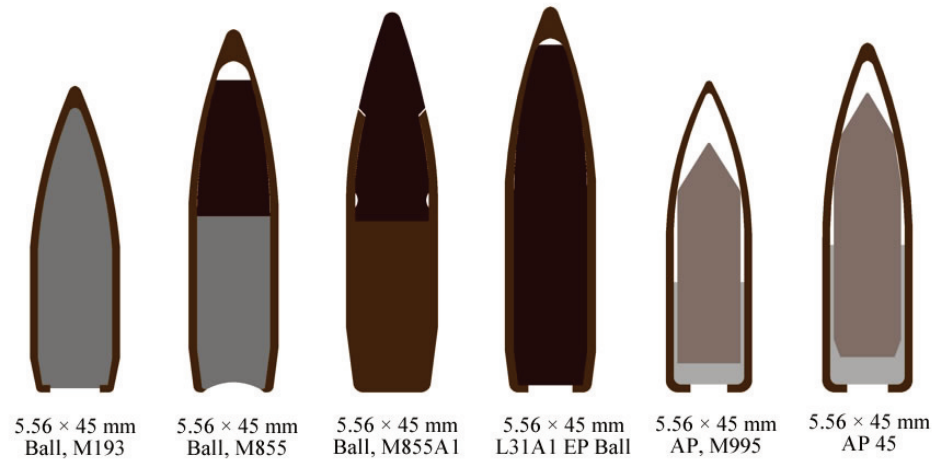

Fig. 1 3D model cross-sections of different 5.56 × 45 mm projectiles, used in research

The early M16 assault rifle and several other weapons (early models of the Galil, FAMAS, HK 33, and SG-540) were all chambered in the 5.56 × 45mm Ball, M193 cartridge. It uses a more fouling propellant, has a longer twist barrel, a lighter projectile (3.6 g), and a higher muzzle velocity than the upgraded 5.56 × 45 mm NATO bullet. The US Army recognized and type-standardized this cartridge in 1963. The cartridge is designed to be used against unarmored targets and troops. It is identified by a plain bullet tip. The initial velocity of the projectile (Fig. 1) is 990 m/s at 4 m

from the muzzle [36, 37]. This greatly depends on the weapon's barrel length. M193 is not designed for long-range precision shooting (M193 is considered to be accurate enough for combat use out to around 500 m). When M193 hits soft tissue, it begins to yaw or tumble. So, when the projectile is traveling fast enough, this often results in the projectile tearing itself apart at the cannelure, which is the weakest part of the projectile. Fragmentation of the projectile usually occurs above the impact velocity of 820 m/s into the soft tissue – for a (508 mm) barrel this corresponds to an approximate distance of 180 m [24, 38]. The ballistics table for this projectile can be found in [24].

The 5.56 × 45 mm, Ball, SS109/M855 cartridge, with a standard 4 g lead core projectile (spitzer boat-tail type, Fig. 1) and hardened steel penetrator, can penetrate 38-51 cm into soft tissue but it can yaw in human tissue. It may, however, yaw and then fracture at the cannelure (the crimping groove surrounding the projectile body) with impact speeds more than 760 m/s. These small pieces have the ability to penetrate both tissue and bone, causing more harm. When fragmentation happens, human tissue is damaged more severely than bullet size and speed would indicate. Since barrel length and velocity have a significant influence on the fragmentation effect, short-barreled carbines lose their ability to inflict wounds at longer ranges than rifles with longer barrels because they produce less muzzle velocity. Compared to the older 5.56 × 45 mm M193 model, the SS109/M855 uses a heavier and more effective bullet, a cleaner propellant, has a lower muzzle velocity and uses a faster rifling twist rate (1:7" twist barrel) [39]. The velocity retention is also improved compared to M193. Projectile for this cartridge can be classified as a semi-armor piercing type. According to standard [40], the average velocity of the projectile should be 914.4 m/s ± 12.2 m/s at 2.4 m from the weapon muzzle. Other data suggests that an initial velocity is 922 m/s at 23.8 m from the muzzle [41]. With common assault rifles, typical muzzle velocity is between 900 and 960 m/s. It is required that a projectile perforate a mild steel plate of 3.5 mm nominal thickness, placed at 570 m from the muzzle at 0° obliquity (normal to the line of fire) [40]. The minimum energy must be ≥ 1 564 J (1 480 J at 24 m from the muzzle). The projectile components are gilding metal jacket, lead core (slug), and hardened steel penetrator in front of the lead slug. The projectile consists of approximately 53 % lead, 46.5 % steel, and 0.5 % antimony [42]. It can be used with 5.56 mm M249E1 machine gun, 5.56 mm M16A2 rifle etc. It is intended for use against personnel and unarmored targets. The cartridge is identified by a green projectile tip [41]. Ballistics table for this projectile can be found in [24]. The aerodynamic and flight dynamic characteristics of the M855 projectile can be found in [43].

In June 2010, the 5.56 × 45 mm, Ball, M855A1 Enhanced Performance Round (EPR) was unveiled, taking the place of the M855. The US Army's goal to field a cartridge better than M855 and the development of a lead-free, "eco friendly" ammunition are combined to create the M855A1. It is designed for use in rifles with shorter barrels (M4 carbine). The M855A1 offers improved hard target capability, more consistent performance at all distances, enhanced dependability, improved accuracy, reduced muzzle flash, and higher velocity compared to the SS109/M855 round. The M855A1 round's new (4 g) projectile features a hardened steel "stacked-cone" penetrator atop a copper core. The jacket reveals its bare steel tip. Originally intended to be made of a tin/bismuth alloy, copper was chosen instead after it was discovered that the alloy did not have enough mass to stabilize the projectile. Because the M855A1 cartridge fires a lead-free projectile, it is frequently referred to as "green ammo" (Fig. 1). A 9.5 mm thick mild steel target may be penetrated by the EPR at 350 m by an M4 and 400 m by an M16 rifle (vs 160 m for M855).

The M855A1 muzzle velocities are raised to 960 m/s (+11 m/s) for the M16 and 910 m/s (+16 m/s) for the M4 carbine in comparison to the SS109/M855. The SS109/M855 projectile is 3.2 mm shorter than the M855A1 projectile. The bullet is stretched within the casing to equal the previous bullet's mass since lead is denser than steel and copper. This cartridge's projectile is categorized as semi-armor penetrating. The M855A1 has a superior combination of penetration, barrier blind characteristics, and terminal efficacy against soft targets, while the M855, however useful in extending the effective range of earlier 5.56 mm projectiles, is no longer in production.

The 5.56 × 45 mm, Ball, L31A1, Enhanced Performance (EP) is a new cartridge, developed by BAE Systems, with enhanced penetration capability. It is compatible with all 5.56 mm NATO weapons and has removed all lead from the projectile (green ammo). This cartridge provides increased firepower from existing weapons. Projectile with a mass of 4 g (Fig. 1) consists of gilding metal jacket enveloping a hardened steel core. While this projectile retains the overall shape and 4 g mass of the M855A1 projectile, armor penetration is increased [37, 44].

Cartridge 5.56 × 45 mm, AP, M995 (designated as AP3 round by Nammo AS [45]) is lead-free, armor piercing (AP) cartridge (designed in 1996), identified by black paint at the projectile tip. The mass of the projectile is 3.4 g, and the velocity is 1 013.2 m/s at 23.8 m in front of the muzzle [41]. Other data suggests velocity of 1 030 m/s, with muzzle energy of 1 750 J. Projectile for this cartridge (Fig. 1) consists of tungsten carbide core (density around 14.5 g/cm^3 [46], hardness 1 200-1 500 HV) encased with aluminum core casing (sleeve), and gilding metal jacket. Cermet composites, which are employed for these projectile cores, are made of dispersed tungsten carbide particles and a metallic matrix, commonly based on cobalt (toxic element). Liquid-phase sintering is used to create these composite materials. The most significant characteristics that define them are high hardness, strong compressive and bending strength, and a comparatively high density [10]. In addition, this projectile offers improved penetration performance against various targets (capability to penetrate lightly armored vehicles at extended ranges) compared to standard 5.56 × 45 mm Ball ammunition. This cartridge can be used with 5.56 mm M16A2 rifle, M4 carbine, M249 Squad Automatic Weapon (SAW), etc. [41]. Projectile penetrates 12 mm of rolled homogeneous armor (300 HB) at 100 m (normal incidence angle) and light body armor at normal combat distances. To determine the effectiveness of 5.56 × 45 mm M995 cartridge, MIL-PRF-7120A (AR) is used.

Nammo AS developed a heavier version of a similar projectile, namely 5.56 × 45 mm, Armour Piercing 45 (AP45; Fig. 1) cartridge, which significantly improves performance at longer ranges in comparison with its lighter counterpart, AP3. The shape of the AP45 penetrator is slightly different than that of AP3 penetrator [47]. In addition to being longer, it has a chamfered base and an ogive front section with two distinct radiuses to prevent the core from rotating in relation to the projectile's rest. Projectile has a mass of 4.5 g and a muzzle velocity of 900 m/s. It penetrates the NATO plate at 900 m, and 7 mm RHA at 200 m [48].

In terms of general military use, the 5.56 × 45 mm NATO ammunition is generally considered the replacement for the 7.62 × 51 mm NATO. Throughout the Vietnam War, they were the preferred infantry cartridge. When comparing the 5.56 × 45 mm NATO to the 7.62 × 51 mm NATO, the higher beginning velocity of the former somewhat compensates for the projectile's limited mass due to its higher kinetic energy. The military still uses the more powerful 7.62 × 51 mm NATO because of its great kinetic force and range. For heavier belt-fed medium machine guns (M60, MG3, FN

MAG), which are used by infantry weapons squads, weapons platoons, and as vehicle-mounted support weapons, 7.62 × 51 mm NATO ammunition is still the norm. Furthermore, specific sniper rifles continue to use this bullet for longer ranges. Even at moderate ranges, 7.62 × 51 mm usually outperforms the 5.56 × 45 mm, penetrating deeper and transferring more energy (even though lethality generally depends on the projectile type, its mass, and impact velocity). This comes at a cost: larger cartridge length and mass, as well as larger recoil and muzzle rise in the case of 7.62 × 51 mm. On the other hand, 5.56 × 45 mm is a great close-quarters fighting ammunition (also sports competitions) and has a lower risk of over-penetration, should a miss occur. The 5.56 × 45 mm ammunition is shorter in length and thus lighter to carry (with a larger number of cartridges for the same mass – a 10 kg loadout of 5.56 × 45 mm is about 660 rounds while 10 kg of 7.62 × 51 mm is about 280 rounds, including magazines). Because 5.56 mm ammunition is smaller, lighter, and more compact, rifles and squad automatic weapons can be used. Moreover, a 5.56 × 45 mm cartridge costs less than a 7.62 × 51 mm cartridge. An unparalleled level of lethality and downrange effect is available to infantrymen using contemporary 5.56 mm ammunition due to its lightweight, low recoil, increased accuracy, longer range, and improved terminal ballistics.

4 Numerical Simulations

4.1 Introduction

Ansys Workbench's Autodyn Lagrange processor was used in the study's simulations. The hydrocode Autodyn is capable of applying finite-element, finite-difference, and finite-volume techniques to solve time-dependent problems involving geometric and material nonlinearities. The Lagrange processor usually uses a structured (I-J-K) numerical mesh made up of brick components (3D) or quadrilaterals (2D). The vertices of the mesh follow the material flow rate exactly. Since the Lagrange formulation does not need to compute material movement across the mesh, it is computationally faster than the Eulerian approach.

On the one hand, the Lagrange framework helps explain free surfaces, material interfaces, and history-dependent material behavior. On the other hand, its main drawback of is that excessive material movement may cause the numerical mesh to become severely distorted, which could lead to an inadequate solution and the calculation ceasing. Rezoning the mesh involves projecting the distorted solution onto a regular mesh, which is one method of correcting mesh distortion. Furthermore, Autodyn offers additional techniques, like erosion, to expand the Lagrange formulation to extremely distorted phenomena. The partial differential equations that must be solved in the Lagrange processor express the conservation of mass, momentum, and energy in Lagrangian coordinates. These, along with a material model and a set of initial and boundary conditions, define the problem's complete solution [49].

4.2 The Numerical Model Validation

The validation of the numerical model was performed using experimental data publicly available. Namely, a limit velocity (maximum velocity at which there is no penetration of target plate) of the 9 × 19 mm, Ball, Parabellum projectile, when impacting 1.2 mm target plate (aluminum alloy, 2024-T3), was determined using simulations and compared to the results presented in the paper of Hub et al [35]. In

[35], this ballistic limit had the value of 95 m/s (condition: projectile doesn't penetrate aluminum sheet and debris occurs).

In this research, a CAD model of a target and a 9 × 19 mm, Ball projectile was first made using CAD software, and then it was exported as .iges file so it could be imported into the Explicit Dynamics module of Ansys Workbench. Fixing the target on its outer edge (parallel to the symmetry axis) was the boundary condition. The target's dimensions were 200 mm in diameter and 1.2 mm in thickness (as in [35]). The projectile's rotation velocity was not taken into account in the simulations.

Three different meshes were used: basic, fine, and very fine. Basic mesh parameters were: face elements size 0.1 mm. Fine mesh parameters were: elements size 0.08 mm. Very fine mesh parameters were: elements size 0.05 mm.

The material models for the projectile components – the core and the casing/gilding metal jacket – were obtained from [35] and the Autodyn material library. For the target plate, they were also obtained from reference [35].

The Gruneisen shock equation of state was applied to the target plate (aluminum alloy 2024-T3), with the constants: $\rho = 2\,770$ kg/m^3, $\Gamma = 2.0$, $c_0 = 5\,328$ m/s, and $s = 1.338$. The Johnson-Cook model was utilized to create the constitutive model for the target, with the constants A = 369 MPa, B = 684 MPa, n = 0.73, C = 0.0083, and m = 1.7. The Johnson-Cook damage model was used as the failure model for the target, and its constants were $D_1 = 0.112$, $D_2 = 0.123$, $D_3 = 1.5$, D_4=0.007, $D_5 = 0$ [35]. For lead core and gilding metal jacket (chosen as equivalent to copper), the Gruneisen shock equation of state parameters (obtained from Autodyn library) are as follows: copper ($\rho = 8\,930$ kg/m^3, $\Gamma = 2.02$, $c_0 = 3\,940$ m/s, $s = 1.489$), lead ($\rho = 11\,340$ kg/m^3, $\Gamma = 2.74$, $c_0 = 2\,006$ m/s, and $s = 1.429$).

Table 1 shows the parameters of the strength model (Steinberg-Guinan) in simulations for the lead core and gilding metal jacket (material equivalent to copper in Autodyn). The author's earlier work [50] has more information on the Steinberg-Guinan constitutive model and shock EOS model. Erosion in numerical simulations was controlled with geometric strain (a default value of 1.5 was chosen), and material failure (defined for target). Eroded elements retained their inertia during simulations.

Tab. 1 Parameters of Steinberg-Guinan strength model utilized in simulations for projectile lead core and gilding metal jacket materials (Autodyn library)

Material	Shear modulus [MPa]	Yield stress [MPa]	Max. yield stress [MPa]	Hardening constant and exponent	Derivative dG/dP	Derivative dG/dT [MPa/K]	Derivative dY/dP
Lead (core)	8.6×10^3	8.0	1×10^2	110; 0.52	1.00	−9.976	-9.3×10^{-4}
Copper (jacket)	4.77×10^4	1.2×10^2	6.4×10^2	36; 0.45	1.35	−17.980	0.003396

Qualitative explanations of obtained results with four different meshes are summarized in Tab. 2. As it can be seen, fine and very fine meshes (element size 0.05-0.08 mm) provide the best agreement with the results from [35], namely ballistic limit with the value of 95 m/s (projectile does not penetrate aluminum sheet and debris occurs, as in [35]). Even though fine meshes demand more computer resources and take more time for simulation to finish, these types of meshes are recommended for

small-caliber projectiles, and are used further in this research. A similar conclusion, regarding mesh size recommendation, was reported in [9].

Tab. 2 Qualitative explanations of phenomena observed with four different meshes (for 9 × 19 mm, Ball, Parabellum projectile)

Projectile impact velocity		
95 m/s	100 m/s	105 m/s
Description of phenomena observed		
Basic (0.1 mm) mesh		
no perforation (rebounding of the projectile from target)	fracture of the target with no projectile passing	perforation with projectile passing (central plug discarded forward from target)
Fine (0.08 mm) mesh		
no perforation (rebounding of the projectile from target, target starts cracking and some debris)	fracture of target with no projectile passing (central plug discarded from target)	perforation with projectile passing (central plug discarded forward from target)
Very fine (0.05 mm) mesh		
target fracture with no projectile passing (rebounding of projectile from target; central plug discarded from target; more debris visible)	perforation with projectile passing (central plug discarded from target; large debris field)	perforation with projectile passing (central plug discarded forward from target; further increased debris field)

4.3 Penetration Capability of Several 5.56 × 45 mm Projectiles into Hard Targets

In this section, six types of 5.56 × 45 mm projectiles will be the subject of the analysis where the impact velocity has been chosen to be 900 m/s for all models (note that real initial velocity of these projectiles is equal (AP45 model) or larger (all other models) than 900 m/s). This should allow evaluation of the effect of the projectile design (the same caliber) on the effectiveness of the projectile when fired against a hard steel target (using the same impact velocity).

Numerical simulations of 5.56 × 45 mm projectile impacts on hard steel targets (Armox 500T steel) were conducted as an essential part of these analyses. With a nominal 500 HBW hardness, Armox 500T is a high-hardness armor steel with extraordinary toughness capabilities that can be used in buildings, automobiles, and a variety of other applications. Armox 500T is not intended for further heat treatment. Popławski [51] reports on important mechanical parameters for Armox 500T steel: hardness 480-540 HBW, yield strength 1 250 MPa, tensile strength 1 450-1 750 MPa. This steel is composed of 0.32 % C, 0.4 % Si, 1.2 % Mn, 0.015 % P, 0.01 % S, 1.01 % Cr, 1.81 % Ni, 0.7 % Mo, and 0.005 % B. Table 3 lists the generic materials and projectile parts used in numerical simulations.

Based on their geometry, a 2D model of the target and projectiles was made in CAD software and exported as .iges file needed for Explicit Dynamics module of Ansys Workbench. The Lagrangian method was utilized to discretize the 2D axisym-

metric models into fine mesh elements (0.05 mm size). The projectile velocity, or impact velocity, was the initial condition. It was 900 m/s for all projectiles in the analysis. Fixing the target on its outer edge (parallel to the symmetry axis) was the boundary condition. The target was 200 mm in diameter and 15 mm in thickness.

Tab. 3 Projectile components and materials used in simulations

Caliber/Model		Projectile components and materials used in simulations
5.56 × 45 mm	Ball, M193	core (lead), jacket (copper)
	Ball, M855	core (lead), jacket (copper), penetrator (hardened steel)
	Ball, M855A1	core (copper), jacket (copper), penetrator (hardened steel)
	Ball, L31A1	jacket (copper), penetrator (hardened steel)
	AP, M995	cup (aluminum), jacket (copper), penetrator (tungsten carbide)
	AP45	cup (aluminum), jacket (copper), penetrator (tungsten carbide)

Generally, two distinct components make up material deformation: the volumetric response, which involves volume changes (equation of state, or EOS), and the deviatoric response, which involves shape changes (strength constitutive model). Since materials can only withstand a certain amount of stress or deformation, it is sometimes required to provide a failure model.

Projectile component materials are listed in Tab. 3 and parameters used in simulations (for strength, EOS, and failure model) are listed in Tabs 4-6. Table 1 in the previous Section of the paper presents the Steinberg-Guinan constitutive model parameters for lead and copper that were used in all numerical simulations. Element erosion in simulations was controlled with geometric strain parameter (Autodyn default value of 1.5 for all components), and material failure (defined for target). Also, eroded elements retained their inertia in the simulations.

Note that projectile material models used in these simulations (Tabs 4-6) do not necessarily accurately represent materials used in commercially available projectiles from this research. Every company has its standard for materials of projectile components and every material used in real projectiles should first be calibrated (using tests) with particular sets of constants for given material if that material is to be used in high-fidelity numerical simulations.

Tab. 4 Shock EOS data for projectile components material used in simulations

Material	Density [g/cm^3]	Gruneisen coefficient	c_0 [m/s]	s [–]	Specific heat [J/(kg · K)]
Lead [Autodyn library]	11.34	2.74	2006	1.429	124
Copper OFHC [Autodyn]	8.93	2.02	3940	1.489	383
Steels [Autodyn library,34]	7.85	1.93	4570	1.49	455
Aluminum 2024-T3 [35]	2.77	2.0	5328	1.338	875
Tungsten carbide [52]	14.5	1.05	5253	1.11	250

Table 7 presents data for 5.56 × 45 mm projectiles, used in the analysis with same impact velocity (900 m/s), including projectile model/caliber, impact velocity (chosen

arbitrarily in simulations in order to compare design of projectiles), mass of projectiles (determined from CAD models), cross-sectional area, kinetic energy, kinetic energy density (ratio of projectile kinetic energy to cross-section area), and sectional density (ratio of projectile mass to cross-section area).

Tab. 5 Constitutive Johnson-Cook model for target (Armox 500T), tungsten carbide, aluminum and hard steel used in numerical simulations

Material	A [MPa]	B [MPa]	n [–]	C [–]	m [–]
Tungsten carbide [53]	3 000.0	89 000	0.650	0.00000	1.000
Aluminum 2024-T3 [35]	368.5	683.9	0.730	0.00830	1.700
Hardened steel [34]	1 900.0	1 100	0.065	0.05000	1.000
Armox 500T steel [54]	1470.0	702	0.199	0.00549	0.811

Tab. 6 Constants for the Johnson-Cook failure model for target material

Material	D_1	D_2	D_3	D_4	D_5
Armox 500T steel [55]	0.04289	2.1521	−2.7575	−0.0066	0.86

Tab. 7 Data for projectiles in simulations with same impact velocity (900 m/s)

Caliber/Model		v_{impact} [m/s]	m_{proj} [g]	A [mm^2]	E_{kin} [J]	$E_{kin\_density}$ [J/mm^2]	Sectional density [g/mm^2]
5.56 × 45 mm	Ball, M193	900	3.62	24.28	1466	60.38	0.149
	Ball, M855	900	4.07	24.28	1649	67.89	0.168
	Ball, M855A1	900	3.97	24.28	1608	66.22	0.164
	Ball, L31A1	900	3.95	24.28	1600	65.89	0.163
	AP, M995	900	3.38	24.28	1369	56.38	0.139
	AP45	900	4.33	24.28	1754	72.23	0.178

Penetration depths into a given target (Armox 500T steel) for different projectiles, obtained in numerical simulations, are presented in Tab. 8. The final penetration depths can be seen in Fig. 2.

Tab. 8 Penetration depths for different 5.56 × 45 mm *projectiles, obtained in simulations (mesh element size* 0.05 mm*), with the same impact velocity* (900 m/s)

Caliber/Model		Penetration depth [mm]
5.56 × 45 mm	M193	3.7
	M855	6.9
	M855A1	10.4
	L31A1	13.8
	M995	11.1
	AP45	15 (stuck in target)

As a result of numerical simulations, for the same impact velocities (900 m/s) of 5.56 × 45 mm projectiles, the AP45 model showed the highest penetration depth into a given target (Armox 500 T), namely the projectile penetrated the target (15 mm; Tab. 8), but was found stuck in it (Fig. 2) with not enough velocity to pierce through.

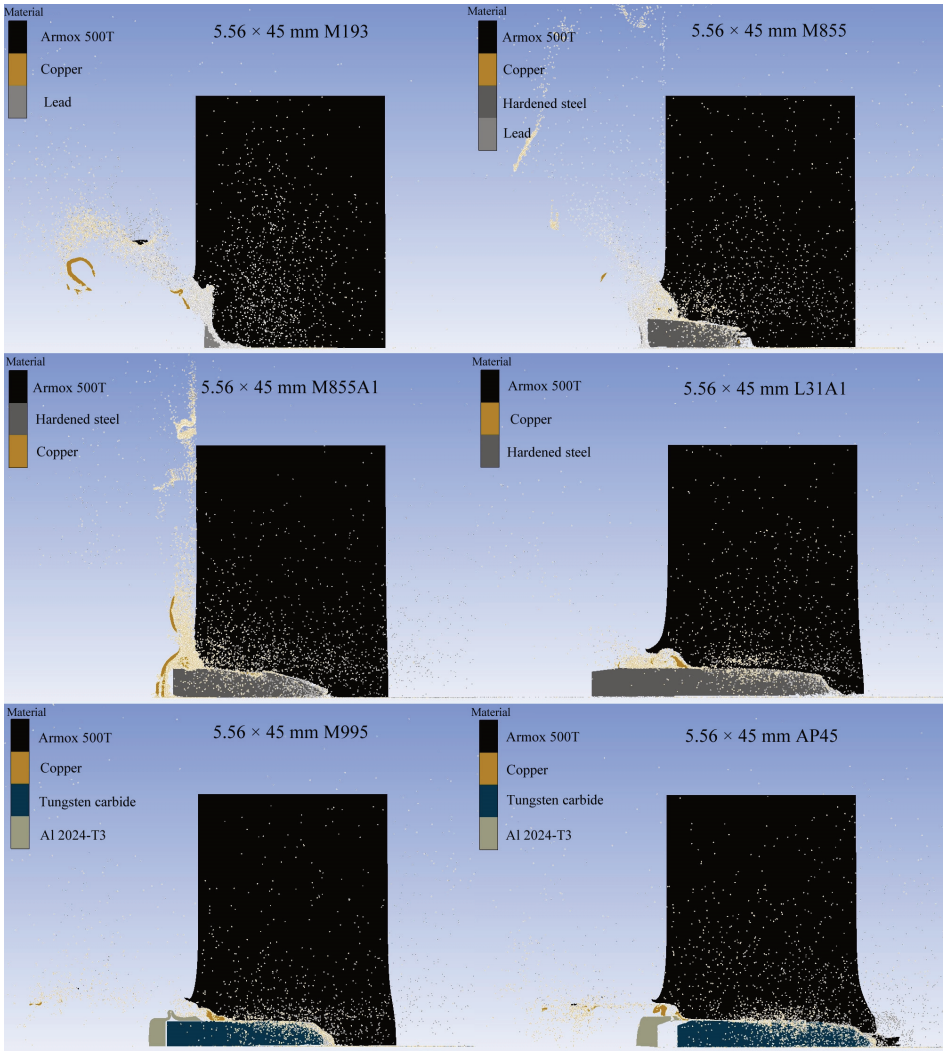

Fig. 2 2D axisymmetric graphic showing penetration depths after 50 μs *(no further penetration observed - limit velocity reached) for* 5.56 × 45 mm *projectiles (M193, M855, M855A1, L31A1, M995 and AP45); velocity* 900 m/s*; element size* 0.05 mm

AP45 projectile has the highest mass, largest kinetic energy (~1 754 J), highest kinetic energy density, and highest sectional density in this group of projectiles. The entry hole in the target for this projectile was 6.8 mm, among the lowest for given projectiles which means that it utilizes its smaller diameter penetrator more efficiently. This effect of the subcaliber penetrator, albeit on a larger scale, is also used effectively in APFSDS projectiles (i.e. larger caliber ammunition). For a given material and mass,

a long, small-caliber core tends to be more efficient than a short, big-caliber one, because the former can concentrate its kinetic energy on a smaller target area. Also, this projectile uses a tungsten carbide penetrator of high density and hardness. It is known that the most effective small-caliber AP projectiles are constructed using cemented tungsten carbides. But despite being less efficient, hardened alloy steel penetrators are still more often employed since they are more affordable and environmentally friendlier [11].

A good example of a relatively efficient hardened steel penetrator projectile is model L31A1 EP with a penetration depth of 13.8 mm observed in simulations. This projectile has a steel penetrator along the whole projectile length, which contributes to increased penetration length compared to projectiles M855 (penetration depth 6.9 mm) and M8855A1 (penetration depth 10.4 mm) which have significantly shorter steel penetrators (150 % and 63 %) in front of lead and copper cores, respectively.

The M995 armor-piercing projectile showed a penetration depth of 11.1 mm into the given target. This projectile (Tab. 7) has, for a given velocity (900 m/s), the lowest kinetic energy (~1 370 J) of all projectiles considered – due to its lowest mass – but it compensates for this disadvantage with its design (sub-caliber penetrator) and penetrator material (dense and very hard tungsten carbide). The entry hole in the target for this projectile was 6 mm, the lowest for given projectiles (utilizes penetrator efficiently) which is expected since its hard and dense penetrator is of smaller diameter compared to other models (except in the AP45 projectile).

Tungsten carbide penetrator armor-piercing projectiles (AP45 and M995), as expected, showed great hard-target penetration capability because of the potent combination of their penetrator material type (dense, hard tungsten carbide), and shape (diameter smaller than other penetrators). It is known in impact dynamics that the denser, harder, and smaller-diameter the penetrator is, other parameters being the same, the greater the penetration depth. Since projectiles with hard steel penetrators typically cannot penetrate ceramic armor, armor-piercing projectiles normally have cemented tungsten carbide cores (generally with a Ni or Co binder). This is partly because the former can penetrate ceramic-faced armor. Tungsten carbide is, on average, 1.85 times denser and significantly harder than hardened steel. However, compared to steel, their manufacturing method is more costly. Tungsten carbide is primarily a fine gray powder, but it can be used by sintering it into shapes and pressing it into place. Inhaling impact dust is the main health danger connected to cemented tungsten carbide, but cobalt's carcinogenic potential should also be taken into account, particularly at shooting ranges.

The lowest penetration depth (3.7 mm) into hard target is observed for the lead-core M193 projectile. However, with this projectile (10.6 mm), the entrance hole in the target was the largest. This is expected since this projectile is mainly used for soft targets (notice the large splash of lead particles during penetration in Fig. 2).

If, for the same impact velocity (900 m/s), projectiles (caliber 5.56 mm) of similar design are compared, i.e. semi-armor piercing projectiles M855 and M855A1, which differ (Fig. 1) in the construction of the frontal part of the jacket (M855A1 does not have a gilding metal jacket on the ogive part), the shape of the penetrator (blunted shape in the M855 compared to the pointed double stacked shape in the M855A1) and the core material (copper in M855A1 instead of toxic lead in the M855), it can be concluded that the M855A1 has a significantly higher penetration depth (around 50%) in a given hard target (Armox 500T). In these projectiles (M855 and M855A1), hard steel is the designated penetrator material. Generally speaking, the penetrator of AP

ammunition is frequently made from steels, including bearing steels, cold-work tool steels, and high-speed tool steels. Due to their lower cost and quick environmental degradation, steel projectile penetrators are employed commonly even though their ballistic effectiveness is significantly lower than that of tungsten carbide penetrators [11]. Steel penetrator in M855A1 is somewhat heavier than steel penetrator in M855 projectile (~45 %) and significantly longer (~54 %). This contributes to an increase in penetration even though M855 is a slightly heavier projectile (~3 %). Also, the lead core of the M855 is around 38 % heavier than the copper core of the M855A1 projectile. Projectile M855 also makes a larger entry hole in the target (Fig. 2). This process uses up some of the projectile energy which can reduce the penetration depth compared to the M855A1 projectile. Nonexistent gilding metal jacket in the frontal ogive part of the M855A1 projectile seems to reduce the energy spent on stripping the jacket (Fig. 2) of the projectile (process generally seen in all FMJ projectiles) which can potentially increase the penetration capability of the given projectile. Simulations also showed that the copper core of the M855A1 does not deform as much during penetration as the lead core of the M855 because copper is a stronger material than lead.

If, for the same impact velocity (900 m/s), 5.56 × 45 mm M995 and AP45 armor-piercing projectiles are compared, which have a similar overall design and the same materials used, it can be concluded that the AP45 model, which has a longer penetrator (by 20 %) with similar diameter values, and a larger mass (by 28 %), allows greater penetration of a given target (35 % in this case). Generally, it is known that greater mass and length of penetrator increase penetration depth, all other parameters being kept the same.

Projectiles M193 and L31A1 projectiles are, generally, of similar overall design, with M193 containing a full lead core, and L31A1 containing a full hard steel core inside a gilding metal jacket. But lead is a significantly weaker material than steel which is shown in their penetration capability. Namely, L31A1, for a given target, shows a 273 % (or 3.73×) increase in penetration depth compared to M193, for the same impact velocity (900 m/s). Naturally, they have different roles in combat, M193 being mainly used against soft targets and L31A1 against harder targets.

5 Conclusions

In the paper, six popular types of 5.56 × 45 mm projectiles (M193, M855, M855A1, L31A1, M995, and AP45) were analyzed. Each projectile had the same impact velocity of 900 m/s. As a result, it was possible to evaluate the effect of each projectile design (and materials) on its efficacy against a hard steel target. This type of terminal ballistics analysis and comparison of a larger number of real contemporary projectiles could not be found in publicly available literature.

Numerical simulations (Ansys Autodyn) of the penetration capability of six projectiles on hard steel targets (Armox 500T steel) were run as part of these analyses. Numerical model was first validated with available experimental data.

The results of the numerical simulation analyses in the research revealed the following:

- the 5.56 × 45 mm AP45 projectile showed a significant increase in penetration depth for a particular hard steel target (Armox 500T), namely ~305 % compared to the M193, ~117 % compared to M855, ~44 % compared to M855A1, ~35 % compared to M995 projectile, and ~9 % compared to L31A1 projectile,

- projectile design has a large impact on its penetration capability. For example, smaller diameter penetrators offer an increase in penetration depth, with other parameters being the same. Similarly, penetrators with larger lengths increase the penetration capability, with other parameters being kept constant,
- projectile materials have also a profound impact on their penetration capability – denser and harder penetrators offer significant increases in penetration depth, other parameters being held constant,
- nonexistent gilding metal jacket in the frontal ogive part of the projectile can reduce the energy spent on stripping the jacket of the projectile which can potentially increase the penetration capability of the projectile,
- the M193 projectile, with soft lead core and gilding metal jacket, shows significantly lower penetration depths into hard targets, compared to other projectiles, which was expected. But it also gives a larger entry hole because of the larger deformation of lead core. This projectile is mainly used against soft targets.

Additional investigation may be focused on examinations of other significant factors that impact the penetration capacity of projectiles with small calibers, such as impact parameters (angle of incidence, target layout, target material types, stacked targets, inclined targets, etc.).

Also, focus might be given to better characterize the projectile components materials failure models in order to be able to use them in high-fidelity numerical simulations in the future. For this task, dynamic experiments have to be performed where particular constants in the models should be calibrated for given material.

References

[1] LEEDER, J. *Armor Piercing Bullets with Sintered Carbide Cores* [online]. 1941 [viewed 2024-02-02]. Available from: https://apps.dtic.mil/sti/tr/pdf/AD0702256.pdf

[2] HAZELL, P.J., M.J. IREMONGER, P.C. BARTON and J.P.F. BROOS. Anomalous Target Failure at Small Angles of Obliquity. In: *21st International Symposium on Ballistics*. Adelaide: Adelaide Convention Centre, 2004, pp. 928-934. ISBN 978-0-9752028-0-7.

[3] FLORES-JOHNSON, E., M. SALEH and L. EDWARDS. Ballistic Performance of Multi-Layered Metallic Plates Impacted by a 7.62-mm APM2 Projectile. *International Journal of Impact Engineering,* 2011, **38**(12), pp. 1022-1032. DOI 10.1016/j.ijimpeng.2011.08.005.

[4] KILIÇ, N. and B. EKICI. Ballistic Resistance of High Hardness Armor Steels Against 7.62 mm Armor Piercing Ammunition. *Materials and Design*, 2013, **44**, pp. 35-48. DOI 10.1016/j.matdes.2012.07.045.

[5] KILIÇ, N., B. EKICI and S. HARTOMACIOĞLU. Determination of Penetration Depth at High Velocity Impact Using Finite Element Method and Artificial Neural Network Tools. *Defence Technology*, 2015, **11**(2), pp. 110-112. DOI 10.1016/j.dt.2014.12.001.

[6] WIŚNIEWSKI, A. and D. PACEK. Flexible Modular Armour for Protection Against the 5.56 × 45 mm SS109 Projectiles. *Problems of Mechatronics Armament, Aviation, Safety Engineering*, 2015, **2**(20), pp. 21-40. DOI 10.5604/20815891.1157772.

[7] HAZELL, P.J. Numerical Simulations and Experimental Observations of the 5.56-mm L2A2 Bullet Perforating Steel Targets of Two Hardness Values. *Journal of Battlefield Technology*, 2003, **6**(1), pp 1-4. ISSN 1440-5113.

[8] JANISZEWSKI, J., M. GRĄZKA, D.E. TRIA, Z. SURMA and B. FIKUS. Laboratory Investigations on Perforation of 30PM Steel Plates. *Problems of Mechatronics Armament, Aviation, Safety Engineering*, 2016, **7**(2), pp. 19-40. DOI 10.5604/20815891.1203115.

[9] COGHE, F., N. NSIAMPA, L. RABET and G. DYCKMANS. Experimental and Numerical Investigations on the Origins of the Bodywork Effect (K-Effect). *Journal of Applied Mechanics*, 2010, **77**(5). DOI 10.1115/1.4001692.

[10] KOLMAKOV, A.G., I.O. BANNYKH, V.I. ANTIPOV, L.V. VINOGRADOV, and M.A. SEVOST'YANOV. Materials for Bullet Cores. *Russian Metallurgy (Metally)*, 2020, **2021**(4), pp. 351-362. DOI 10.31044/1814-4632-2020-10-8-21.

[11] Di BENEDETTO, G., P. MATTEIS and G. SCAVINO. Impact Behavior and Ballistic Efficiency of Armor-Piercing Projectiles with Tool Steel Cores. *International Journal of Impact Engineering*, 2018, **115**, pp. 10-18. DOI 10.1016/j.ijimpeng.2017.12.021.

[12] ANDERSON, Jr., C.E., V. HOHLER, J.D. WALKER and A.J. STILP. The Influence of Projectile Hardness on Ballistic Performance. *International Journal of Impact Engineering*, 1999, **22**(6), pp. 619-632. DOI 10.1016/S0734-743X(98)00069-4.

[13] TRIA, D.E. and R. TRĘBIŃSKI. Methodology for Experimental Verification of Steel Armour Impact Modelling. *International Journal of Impact Engineering*, 2017, **100**, pp. 102-116. DOI 10.1016/j.ijimpeng.2016.10.011.

[14] ROSENBERG, Z., P. KOSITSKI and E. DEKEL. On the Perforation of Aluminum Plates by 7.62 mm APM2 Projectiles. *International Journal of Impact Engineering*, 2016, **97**, pp. 79-86. DOI 10.1016/j.ijimpeng.2016.06.003.

[15] HAZELL, P.J., G.J. APPLEBY-THOMAS, D. PHILBEY and W. TOLMAN. The Effect of Gilding Jacket Material on the Penetration Mechanics of a 7.62 mm Armour-Piercing Projectile. *International Journal of Impact Engineering*, 2013, **54**, pp. 11-18. DOI 10.1016/j.ijimpeng.2012.10.013.

[16] BØRVIK, T., S. DEY and A.H. CLAUSEN. Perforation Resistance of Five Different High-Strength Steel Plates Subjected to Small-Arms Projectiles. *International Journal of Impact Engineering*, 2008, **36**, pp. 948-964. DOI 10.1016/j.ijimpeng.2008.12.003.

[17] DEY, S., T. BØRVIK, X. TENG, T. WIERZBICKI and O.S. HOPPERSTAD. On the Ballistic Resistance of Double-Layered Steel Plates: An Experimental and Numerical Investigation. *International Journal of Solids and Structures*, 2007, **44**, pp. 6701-6723. DOI 10.1016/j.ijsolstr.2007.03.005.

[18] MOHOTTI, D., T. NGO, S.N. RAMAN and P. MENDIS. Analytical and Numerical Investigation of Polyurea Layered Aluminium Plates Subjected to High Velocity Projectile Impact. *Materials and Design*, 2015, **82**, pp. 1-17. DOI 10.1016/j.matdes.2015.05.036.

[19] HUB, J. and P. KNEYS. 3D Simulation Analysis of Aircraft Protection Material Impacting by 7.62 mm Ammunition, *University Review*, 2013, **7**(3), pp. 15-19. ISSN 1337-6047.

[20] SOYDAN, A.M., B. TUNABOYLU, A.G. ELSABAGH, A.K. SARI and R. AK-DENIZ. Simulation and Experimental Tests of Ballistic Impact on Composite Laminate Armor. *Advances in Materials Science and Engineering*, 2018, **18**, 4696143. DOI 10.1155/2018/4696143.

[21] SIRIPHALA, P., T. VEERAKLAEW, W. KULSIRIKASEM and G. TANAP-ORNRAWEEKIT. Validation of FE Models of Bullet Impact on High Strength Steel Armors. *WIT Transactions on The Built Environment*, 2012, **126**, pp. 75-83. DOI 10.2495/SU120071.

[22] TRIA, D.E. and R. TRĘBIŃSKI. On the Influence of Fracture Criterion on Perforation of High-Strength Steel Plates Subjected to Armour Piercing Projectile. *Archive of Mechanical Engineering*, 2015, **62**(2), pp. 157-179. DOI 10.1515/meceng-2015-0010.

[23] HORSFALL, I., N. EHSAN and W. BISHOP. A Comparison of the Performance of Various Light Armour Piercing Ammunition. *Journal of Battlefield Technology*, 2000, **3**(3), 3-3-2.

[24] KNEUBUEHL B.P, COUPLAND, R.M., M.A. ROTHSCHILD, M.J. THALI. *Wound Ballistics: Basics and Applications*. Berlin: Springer, 2011. ISBN 978-3-642-43589-8.

[25] HUB, J., J. KOMENDA and F. RACEK. The Analysis of Terminal-Ballistic Behaviour of a Pistol Bullet Penetrating a Block of Substitute Biological Material. *Problemy Mechatroniki: Uzbrojenie, Lotnictwo, Inżynieria Bezpieczeństwa*, 2013, **4**(1), pp. 19-35. ISSN 2081-5891.

[26] BØRVIK, T., A.S. HOPPERSTAD, M. LANSETH and K.A. MALO. Effect of Target Thickness in Blunt Projectile Penetration of Weldox 460 E Steel Plates. *International Journal of Impact Engineering*, 2003, **28**(4), pp. 413-464. DOI 10.1016/S0734-743X(02)00072-6.

[27] YIN, G.X., Q. ZHANG, P. CHEN, B.H. HONG, N. JIANG and D.C. GAO. Study of Armor-Piercing Self-Sharpening Properties of 88WC-12Co Material. *Journal of Physics: Conference Series*, 2023, **2478**, 072006. DOI 10.1088/1742-6596/2478/7/072006.

[28] EDWARDS, M.R. and A. MATHEWSON. The Ballistic Properties of Tool Steel as a Potential Improvised Armour Plate. *International Journal of Impact Engineering*, 1997, **19**(4), pp. 297-309. DOI 10.1016/S0734-743X(97)83210-1.

[29] ERZAR, B. and J.L. ZINSZNER. Dynamic Characterization of Tungsten Carbide Behaviour at Very High Strain-Rates. *EPJ Web of Conferences*, 2018, **183**, 02061. DOI 10.1051/epjconf/201818302061.

[30] MUBASHAR, A., E. UDDIN, S. ANWAR, N. ARIF, U.S. WAHEED and M. CHOWDHURY. Ballistic Response of 12.7 mm Armour Piercing Projectile Against Perforated Armour Developed from Structural Steel. *Proc IMechE Part L: J Materials: Design and Applications*, 2019, **233**(10), pp. 1993-2005. DOI 10.1177/1464420718808317.

[31] MUBASHAR, A., E. UDDIN, S. ANWAR, N. ARIF, U.S. WAHEED and M. CHOWDHURY. Ballistic Response of 12.7 mm Armour Piercing Projectile Against Perforated Armour Developed from Structural Steel. *Proc IMechE Part L: J Materials: Design and Applications*, 2019, **233**(10), pp. 1993-2005. DOI 10.1177/1464420718808317.

[32] JOHNSON, Jr., A. E. *Mechanical Properties at Room Temperature of Four Cermets of Tungsten Carbide with Cobalt Binder* [online]. 1954 [viewed 2023-26-12]. Available from: https://www.osti.gov/biblio/4362482

[33] BØRVIK, T., L. OLOVSSON, S. DEY and M. LANGSETH. Normal and Oblique Impact of Small Arms Bullets on AA6082-T4 Aluminium Protective Plates. *International Journal of Impact Engineering*, 2011, **38**(7), pp. 577-589. DOI 10.1016/j.ijimpeng.2011.02.001.

[34] KILIÇ, N., S. BEDIR, A. ERDIK, B. EKICI, A. TAŞDEMIRCI and M. GÜDEN. Ballistic Behavior of High Hardness Perforated Armor Plates Against 7.62 mm Armor Piercing Projectile. *Materials & Design*, 2014, **63**, pp. 427-438. DOI 10.1016/j.matdes.2014.06.030.

[35] HUB, J., J. KOMENDA and M. NOVÁK. Ballistic Limit Evaluation for Impact of Pistol Projectile 9 Mm Luger on Aircraft Skin Metal Plate. *Advances in Military Technology* 2012, **7**(1), pp. 21-29. ISSN 1802-2308.

[36] *5.56 mm (5.56 × 45 mm) Ammunition* [online]. [viewed 2023-11-22]. Available from: https://www.inetres.com/gp/military/infantry/rifle/556mm_ammo.html

[37] *A Survey of Military 5.56* [online]. 2017 [viewed 2023-11-19]. Available from: https://advanceandreview.wordpress.com/2017/05/04/a-survey-of-military-5-56/

[38] *M193 ammunition: Everything You Wanted to Know* [online]. 2003 [viewed 2023-12-19]. Available from: https://battlebornreview.com/m193-ammunition/ [viewed 2023-25-11]

[39] *5.56 × 45 mm NATO* [online]. [viewed 2023-09-25]. Available from: https://weaponsystems.net/system/1513-5.56x45mm%20NATO

[40] *NATO Standard AOP-4172. Technical Performance Specification Providing for the Interchangeability of 5.56 × 45 mm Ammunition* [online]. 2020 [viewed 2024-01-25]. Available from: https://standards.globalspec.com/std/14348976/STANAG%204172

[41] *Army Ammunition Data Sheets - Small Caliber Ammunition FSC 1305* [online]. 1994 [viewed 2024-02-02]. Available from: https://www.armimilitari.it/wordpress/wp-content/uploads/2014/08/tm43-0001-27-small-cartridge.pdf

[42] STEWART, M.G., B. DORROUGH and M.D. NETHERTON. Field Testing and Probabilistic Assessment of Ballistic Penetration of Steel Plates for Small Calibre Military Ammunition. *International Journal of Protective Structures,* 2018, **10**(4), pp. 1-18. DOI 10.1177/2041419618802593.

[43] SILTON, S.I. and B.E. HOWELL. *Aerodynamic and Flight Dynamic Characteristics of 5.56-mm Ammunition: M855* [online]. 2010 [viewed 2023-11-25]. Available from: https://apps.dtic.mil/sti/pdfs/ADA530895.pdf

[44] *Small Arms Ammunition* [online]. [viewed 2023-11-19]. Available from: https://www.baesystems.com/en/product/small-arms-ammunition

[45] *5.56 mm × 45 Armor Piercing 3 (M995)* [online]. [viewed 2024-02-10]. Available from: nammo.com/product/our-products/ammunition/small-caliber-ammunition/5-56mm-series/5-56-mm-x-45-armor-piercing-3/

[46] *Tungsten Carbide Armor Piercing Technology* [online]. 2015 [viewed 2024-02-20]. Available from: https://ndiastorage.blob.core.usgovcloudapi.net/ndia/2015/smallarms/17379_Erninge.pdf

[47] PIASTA, K. and P. KUPIDURA, Perspective Armour-Piercing Intermediate Cartridge Projectile. *Problems of Mechatronics Armament, Aviation, Safety Engineering*, 2023, **14**(1), pp. 89-104. DOI 10.5604/01.3001.0016.2961.

[48] *5.56 mm × 45 Armor Piercing 45* [online]. [viewed 2023-11-25]. Available from: https://www.nammo.com/product/our-products/ammunition/small-caliber-ammunition/5-56mm-series/5-56-mm-x-45-armor-piercing-45/

[49] *AUTODYN® - Explicit Software for Nonlinear Dynamics, Theory Manual - Revision 4.3* [online]. 2005 [viewed 2024-02-03]. Available from: https://www.researchgate.net/profile/Alireza_Rashiddel/post/Is_there_a_way_to_implement_a_large_strain_viscoelastic_material_model_in_AUTODYN/attachment/5f85890de66b860001a8503c/AS%3A946132159045637%401602586893515/download/0-theory_manual_AUTODYN.pdf

[50] CATOVIC, A. Research of Influence of Different Shaped Charge Liner Materials on Penetration Depth Using Numerical Simulations. *Periodicals of Engineering and Natural Sciences*, 2023, **11**(4), pp. 1-26. ISSN 2303-4521.

[51] POPŁAWSKI, A., P. KĘDZIERSKI and A. MORKA. Identification of Armox 500T Steel Failure Properties in the Modeling of Perforation Problems. *Materials & Design*, 2020, **190**, 108536. DOI 10.1016/j.matdes.2020.108536.

[52] HAZELL, P.J, G.J. APPLEBY-THOMAS, K. HERLAAR, and J. PAINTER. Inelastic Deformation and Failure of Tungsten Carbide Under Ballistic-Loading Conditions. *Materials Science and Engineering*, 2010, **527**(29-30), pp. 7638-7645. DOI 10.1016/j.msea.2010.08.024.

[53] HOLMQUIST, T.J., G.R. JOHNSON and W.A. GOOCH. Modeling the 14.5 mm BS41 Projectile for Ballistic Impact Computations. *WIT Transactions on Modelling and Simulation*, 2005, **40**. ISSN 1743-355X.

[54] NILSSON M. *Constitutive Model for Armox 500T and Armox 600T at Low and Medium Strain Rates* [online]. 2003 [viewed 2023-12-21]. Available from: https://www.foi.se/rest-api/report/FOI-R-1068-SE

[55] SENTHIL, K., M.A. IQBAL and S. RUPALI. Influence of Impactor Nature, Mass, Size and Shape on Ballistic Resistance of Mild Steel and Armox 500T Steel. *International Journal of Protective Structures*, 2018, **10**(2), pp. 174-197. DOI 10.1177/2041419618807493.